

## EFFICIENCY ENHANCEMENT OF PHOTOVOLTAIC SOLAR CELLS USING METAMATERIALS ABSORBING SCREEN

Haitham Al Ajmi<sup>1</sup>, Mohammed M. Bait-Suwailam<sup>1,2\*</sup>, Mahmoud Masoud<sup>3</sup>, and Muhammed Shafiq<sup>1</sup>

<sup>1</sup> Department of Electrical & Computer Engineering, Sultan Qaboos University, Muscat, Oman

<sup>2</sup> Remote Sensing & GIS Research Center, Sultan Qaboos University, Muscat, Oman

<sup>3</sup> Department of Electronics & Electrical Engineering, The University of Sheffield, UK

**ABSTRACT:** This paper proposes a novel technique for the efficiency enhancement of photovoltaic (PV) solar cells using metamaterials absorbing screens. This kind of engineered material comprises resonant metallic rings that are printed on a host low-loss dielectric substance and made periodic in a two-dimensional lattice. The absorbing screen has been carefully designed, and its retrieved effective constitutive parameters, effective electric permittivity  $\epsilon_{\text{eff}}$  and effective magnetic permeability  $\mu_{\text{eff}}$ , are integrated within a numerically modelled amorphous-Silicon-based PV solar cell structure as an impedance matching layer. Such arrangement will greatly achieve matching between the effective impedance of the composite solar cell structure and free-space impedance and will result in higher photons absorption through the metamaterials anti-reflective screen. Numerical full-wave electromagnetic simulations are carried out using CST Microwave Studio for the design of a metamaterial absorbing screen. Due to the large computational resources required, COMSOL Multiphysics was adopted in the design and analysis of the composite structure comprising a two-dimensional PV solar cells layer. Based on the numerical results, both optical and electric characteristics of the PV solar cell structure were enhanced with the use of a metamaterial layer. Moreover, efficiency enhancement by 5% was permissible, in which efficiency reached 12% with the use of metamaterials as compared to the efficiency of the classical PV cells of 7%. The obtained results are very promising, and the potential integration of metamaterials in commercial PV solar cells will show significant advancement in efficiency enhancement of PV cells and realization of smart PV solar cells with the consideration of additional features from metamaterials.

**Keywords:** Efficiency, metamaterials, photovoltaic solar cells, renewable energy.

### تعزيز كفاءة الخلايا الشمسية الكهروضوئية باستخدام طبقة من المواد الفائقة العالية الامتصاص

هيثم العجمي، محمد بيت سويلم، محمود مسعود ومحمد شفيق

**المخلص:** تقدم هذه الورقة البحثية طريقة هندسية جديدة لتعزيز كفاءة ألواح الخلايا الشمسية الكهروضوئية باستخدام خصائص المواد الفائقة. هذه المواد الاصطناعية لديها خصائص يتم الحصول عليها من خلال تصميم مثل تلك المواد باستخدام مجسمات معدنية ذات أشكال قابلة للتعرف على الأمواج الكهرومغناطيسية ويتم طباعتها بمواد عازلة. تتركز الدراسة في هذا البحث على تصميم المواد القابلة لامتصاص كمية كبيرة من أشعة الشمس وبالتالي يتم الحصول على كفاءة إضافية للألواح الشمسية. تتطرق الورقة البحثية لطرق المحاكاة باستخدام خوارزميات هندسية لديها القدرة على إيجاد الحلول المثلى للتصميم المقدم، حيث سنقوم بعرض النتائج ومقارنتها بالنتائج المستوحاة من ألواح الخلايا الشمسية. من خلال النتائج التي تم الحصول عليها ومقارنتها بنموذجين من برامج محاكاة الكهرومغناطيسية، تم الحصول على زيادة بكفاءة الألواح الشمسية بنسبة 5% عند استخدام مجسمات المواد الفائقة مقارنة بالألواح الشمسية الاعتيادية.

**الكلمات المفتاحية:** الكفاءة؛ المواد الفائقة؛ الخلايا الشمسية الكهروضوئية؛ الطاقة المتجددة.

## NOMENCLATURE

$A(\omega)$	Absorbance at frequency $\omega$	
$c$	Speed of Light	(m/s)
$FF$	Filling Factor	
$G(z)$	Electron-Hole generation rate	(1/m <sup>3</sup> s)
$h$	Plank's Constant	(m <sup>2</sup> kg/s)
$I$	Solar Cell Output Current	(A)
$I_{max}$	Solar Cell Maximum Current	(A)
$I_o$	Diode Saturation Current	(A)
$I_{ph}$	Photogenerated Current	(A)
$I_{sc}$	Solar Cell Short Circuit Current	(A)
$K(\lambda)$	Extinction Coefficient	
$K_B$	Boltzmann Constant	(m <sup>2</sup> kg/s <sup>2</sup> /K)
$n$	Refractive index	
$P_{in}$	Input Power	(W)
$P_{opt}(\lambda)$	Irradiance Power	(Wm <sup>2</sup> /m)
$q$	Electron Charge	(C)
$R(\lambda)$	Reflectance Coefficient	
$T$	Absolute Temperature	(K)
$T(\omega)$	Transmittance Coefficient at frequency $\omega$	
$V$	Solar Cell Output Voltage	(V)
$V_{max}$	Solar Cell Maximum Voltage	(V)
$V_{oc}$	Solar Cell Open Circuit Voltage	(V)
$\eta$	Solar Cell Efficiency	
$\lambda$	Wavelength	(m)
$\omega$	Frequency	Hz
$\Gamma(\omega)$	Reflectance Coefficient at frequency $\omega$	
$\mu_{eff}$	Effective Permeability	H/m
$\epsilon_{eff}$	Effective Permittivity	H/m
$Z_{eff}$	Effective Impedance	$\Omega$

## 1. INTRODUCTION

In the GCC (Gulf Cooperation Council), the annual predicted electricity demand growth ranges from 5 % to 15 % for all user groups (commercial, residential, and Industrial); e.g., Oman predicts growth from 6 % to 11 %. Hence, new power generation and storage capacity must be constructed, which will lead to consuming more fossil fuels and an increase in CO<sub>2</sub> emissions and energy prices (Ceci *et al.*, 2018; Ferroukhi *et al.*, 2016). The GCC countries have set a target to generate power from renewable energy sources by 2030 with different percentages ranging from 5 % to 30 % to save fuel, reduce CO<sub>2</sub> emissions, reduce power prices, and create job opportunities for their citizens in the renewable energy sector. Figure 1 shows 2030 targets for renewable power generation in the GCC countries. For instance, the United Arab Emirates and Saudi Arabia set the highest goals of 33.3 and 29.3 GW, respectively, while Oman aims to generate around 2.4 GW by 2024 from renewable energy resources. In GCC countries, the primary source of renewable energy is solar cells, followed by concentrated solar cells, with different percentages—e.g., in Oman, 81.6 % of the 2.4 GW planned to be

produced in 2024 will come from solar cells, while 16.3 % from wind power (SAOC, 2018).

Solar photovoltaic (PV) systems technology has reached remarkable growth as one crucial sustainable energy source within the last ten years. PV solar panels utilize the valuable natural green resource, i.e., the sun, to make use of the enormous supply of alternative energy worldwide, despite the variation and availability of the sun and its concentration from one region to another (Ceci *et al.* 2018; Ferroukhi *et al.*, 2016).

Due to the many attractive features of PV solar panels in terms of their reliability, durability, and cost, such technology has been utilized in lots of consumer and industrial applications, including but not limited to green power generation plants, home power supply, industrial, commercial, residential units, to name a few.

However, one major drawback of PV solar cells is their low efficiency (Saga, T. 2010). In fact, the efficiency of PV cells started from 15% in 1950 until it reached 28% in recent years (Saga, T. 2010 & Green, M. 1987). According to the best research findings from the National Renewable Energy Laboratory, NREL (NREL, 2022, Zhang, J. 2016) in solar cells development in terms of efficiency, the highest solar cell efficiency that was reported is around 47.1 % using multi-junction cells, specifically six junctions (Geisz *et al.*, 2020). At the same time, the photovoltaic module with an area ranging from 200-800 cm<sup>2</sup> of the same technology reached up to 40.6% efficiency with outdoor measurements, depending mainly on the applied test conditions. However, this will pose additional design and manufacturing complexity and cost for such kind of multi-junction technology.

Among other techniques that are adopted for PV solar cells efficiency enhancement are photovoltaic thermal techniques, including the use of absorbers (Sathe, T. and Dhoble, A. 2017), maximum power point tracking technique (Chung *et al.*, 2003 & Hohm, D and Ropp, M. 2000), and the extensive investment on materials science to explore methodologies in efficiency enhancement (Biwole *et al.*, 2013 & Zakharchenko *et al.*, 2004).

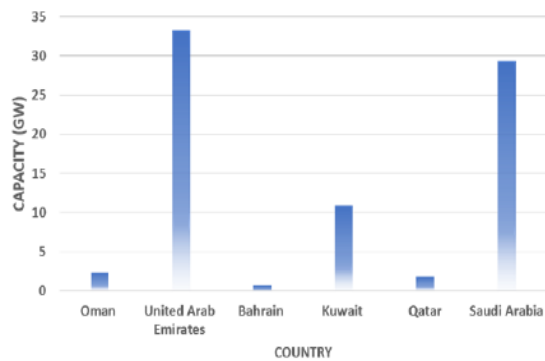


**Figure 1.** Renewable Energy Targets in GCC (2030) and Oman.

Recently, metamaterials have attracted researchers worldwide from science and engineering disciplines. Owing to metamaterials features that cannot be found in ordinary substances, this subject of interest has been explored in the design of microwave devices (Dong, Y. and Itoh, T. 2012; Gil *et al.* 2008 & Alibakhshikenari *et al.* 2018), enhancement of radiating structures, optical lenses (Jiang *et al.*, 2012; Kundtz, N. and Smith, D. 2010 & Zhu *et al.*, 2015), and as an alternative absorbing structure in visible, infrared and optical regimes (Bagmanci *et al.*, 2019; Luo *et al.*, 2017 & Dincer *et al.*, 2014), to name a few. The majority of studies have focused on the design and analysis of metamaterials as absorbers. In the design and synthesis of metamaterials-based energy absorbers, various developments have relied on the use of periodic metallic resonant inclusions that are printed on the dielectric insulating material. For instance, the work in (Shchegiklov *et al.*, 2010), (Baqir, M. and Choudhury P. 2019), and (Wu *et al.*, 2012). The application of metamaterials for the enhancement of PV solar cells has been studied earlier, but from the enhancement of the metamaterials' absorption strength only (Liu *et al.*, 2012, Lin *et al.*, 2020, Hamouche, H. and Shabat, M. 2018). Authors (Liu *et al.*, 2012) presented numerical studies for a groove-based absorber on top of PV solar cell structure using COMSOL Multiphysics. Based on their numerical results, enhancement in photons' absorption was achieved. Another study by (Hamouche, H. and Shabat M. 2018) presented numerical simulations for a three-layer PV solar cell with a metamaterial layer, where the metamaterial layer was embedded between the glass layer (top layer) and the silicon layer. Authors have focused on only optical parameters study, where enhanced light absorption was reported. A number of limitations from previous studies are observed and can be summarized: 1) some of the previous composite structures of PV solar cells with metamaterials have incurred additional complexity in the structure design, 2) earlier attempts on the applicability of metamaterials for PV solar cells have studied the optical parameters of the PV solar cell with metamaterials layer only, while to the best of authors' knowledge, analysis of electrical parameters of PV solar cells with metamaterials have not investigated, and this paper fills the gap for completeness of the study.

In this paper, we focus on the design and development of an efficient, low-cost metamaterials-based anti-reflective screen that is integrated directly on top of PV solar cells. The low-cost term here is referred to the need for fabrication of metamaterials via printed-circuit board technology. By such arrangement, the enhancement of solar cells' efficiency is permissible due to the great matching between solar cells' impedance with free-space impedance.

Our main contributions in this research work can be summarized in the following points: 1) developing an engineered highly absorption metamaterial layer, where its design and results illustrating its effective

impedance matching to free-space are shown, 2) investigating both the optical performance of the PV solar cell with and without the metamaterial layer in terms of photons generation rate and absorption strength and 3) investigating the electrical performance of the PV solar cell ( $I$ - $V$  and  $P$ - $V$  curves) with and without the metamaterial layer, which has not been tackled in previous studies. It is worth noting here that the scope of this research work focuses on the engineering aspects of metamaterials towards enhancement of the overall PV solar cell structure with a metamaterial anti-reflective layer, with a comprehensive study of both optical and electrical parameters.

The rest of the paper is organized as follows. Section 2 briefly outlines some important electrical circuit parameters related to PV solar cells. Section 3 provides a brief overview of metamaterials and our proposed metamaterial absorber structure, and the potential application of embedded metamaterial absorbing screen within PV solar cells. Furthermore, section 3 presents the numerical full-wave simulations and discusses the results. Finally, section 4 concludes the paper with a summary of the findings.

## 2. PV SOLAR CELLS: EQUIVALENT CIRCUIT PARAMETERS

An ideal solar cell could be electrically represented as a current source connected in parallel having a rectifying diode, as illustrated in the equivalent circuit model shown in Figure 2. The related  $I$ - $V$  characteristic is well explained by Schotckley solar panel equations, which are read as (Kalogirou, S., 2017)

$$I = I_{ph} - I_o \left( e^{\frac{qV}{K_B T}} - 1 \right) \quad (1)$$

$$V_{oc} = \frac{K_B T}{q} \ln \left( 1 + \frac{I_{ph}}{I_o} \right) \quad (2)$$

where  $K_B$  is the Boltzmann constant,  $T$  is the absolute temperature,  $q$  is the electron charge,  $V$  is the voltage at the terminals of the cell,  $I_o$  is the diode saturation current,  $I_{ph}$  is the photo-generated current, and  $V_{oc}$  is the open-circuited voltage. Equations (1) – (2) above are essential for the analysis and analytical calculation of the PV solar cell electrical parameters.

Figure 3 depicts the general behaviour of PV solar cells in terms of electrical circuit parameters: output current and power versus biased voltage. Moreover, additional important electrical parameters such as short circuit current ( $I_{sc}$ ), open circuit voltage ( $V_{oc}$ ), maximum power ( $P_{max}$ ), filling factor ( $FF$ ) and efficiency can easily be extracted from the curves. For instance,  $I_{sc}$ ,  $V_{oc}$  and  $P_{max}$  are identified in Figure 3.

The filling factor ( $FF$ ) is a term that is related to the efficiency of PV solar cells and can be calculated from

the following relation:

$$FF = \frac{I_{max}V_{max}}{I_{sc}V_{oc}} \quad (3)$$

where  $I_{max}$  is the maximum current flowing in the PV solar cell junction,  $V_{max}$  is the captured maximum voltage. It is intuitive to then get a unity filling factor for an ideal PV cell.

The efficiency of the PV solar cells can then be calculated using equation (4).

$$\eta = FF \frac{I_{sc}V_{oc}}{P_{in}} \quad (4)$$

where  $P_{in}$  is the input solar power to the PV solar cell, and  $\eta$  is the overall efficiency of the PV solar cell. It is clear from Eqn. (4) that the efficiency of the solar cells is directly related to the filling factor.

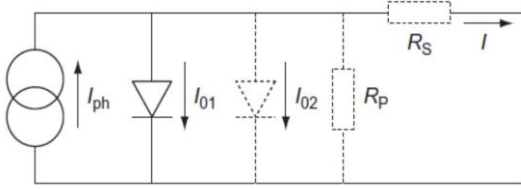


**Figure 2.** Equivalent circuit model for an ideal PV solar cell, along with a non-ideal circuit representation.

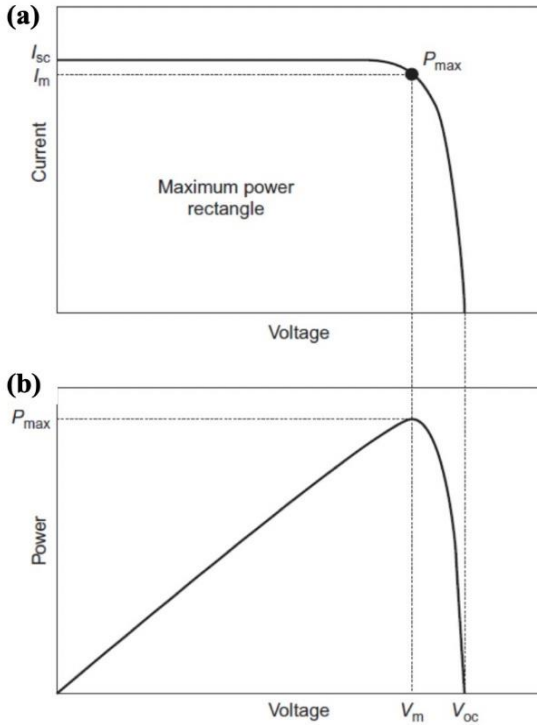


**Figure 3.** PV solar cell electrical parameters representation of: (a) current-voltage curve, and (b) power-voltage curve (Kalogirou, S., 2017).

It is important to highlight here that the above equivalent circuit parameters of PV solar cells are essential to analyze during the numerical full-wave studies. This will provide a complete electrical generation through the migration of electrons via the PV solar junction (Basore, P. 1990 & Brown et al., 2010). An additional study that is essential to be as an input to the electrical study is the light absorption analysis. Through such a study, the hole-electron pair will be generated in a process well-known as the photo-generation rate. This photo-generation can be derived from the Lambert-Beer law (Zimmermann, H. 2000), where the generation rate can numerically be computed using

$$G(z) = \frac{4\pi}{hc} \int_{\lambda_1}^{\lambda_2} (1 - R(\lambda))K(\lambda)P_{opt}(\lambda)e^{-\frac{4\pi K(\lambda)}{\lambda}z} d\lambda \quad (5)$$

where  $h$  is the Planck constant,  $c$  is the speed of light,  $R(\lambda)$  is the reflectance coefficient,  $K$  is the imaginary part of the refractive index at a specific wavelength,  $P_{opt}$  is the spectral irradiance power, and  $z$  is the direction of wave propagation.

### 3. Research Methodology

The adopted research methodology in this work focused on the numerical design and modelling aspects of a developed solar cell integrated with a metamaterial layer for efficiency enhancement.

Firstly, we focus on the design of a low-profile absorber structure for later integration with PV solar cell structure. The design methodology starts up with an initial estimation of resonance through approximate quasi-static relations, after which tuning is carried out within COMSOL Multiphysics. For validation purposes, the same design absorber structure is numerically assessed in CST Microwave Studio. Figure 4 presents the flow chart of the developed solar energy absorber, where involves computing numerically the scattering parameters (reflectance,  $R$ , and transmittance,  $T$ ) of an infinitely large structure from the same absorbing unit cell, and from which one can compute the absorption ( $A = 1 - |R|^2 - |T|^2$ ) and then retrieving the constitutive parameters of the absorbing structure.

Secondly, the performance of the newly developed structure is numerically assessed and compared against a reference PV solar cell without a metamaterials layer. In this work, the research methodology aimed to compute both optical and electrical parameters of the developed PV solar cell structure with a metamaterials layer.

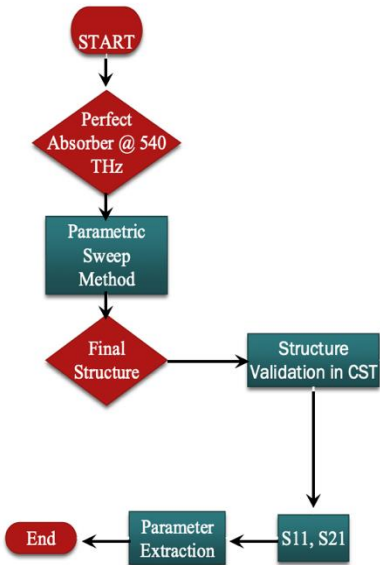


**Figure 2.** Flowchart illustration of the steps carried out through the design of a low-profile solar energy absorber.

#### 4. Metamaterials for renewable energy solutions

Metamaterials are engineered materials that are arranged in a periodic or aperiodic fashion and, when properly designed, can exhibit properties and features not yet observed in nature (Kshetrimayum, R. 2004). In 1968, Victor in (Veselago, V. 1967) studied theoretically the possibility of achieving a negative refractive index, which was possible to realize when negative permittivity materials were realized at the microwave regime in 1999. Smith and his group made the experimental realization of the first double-negative materials, or metamaterials, in 2000 (Shelby *et al.*, 2001).

Metamaterials are frequency-dependent and inherently lossy, which can be tailored to any specific application of interest depending on the desired response of the composite constitutive parameters. It is worth mentioning here that one common way of realizing such small periodic structures can be through printing sub-wavelength resonant metallic inclusions on a host of insulating materials, which can easily be done using low-cost printed-circuit board manufacturing technology. A generic view of a metamaterial structure is depicted in Figure 5, where electrically small metallic resonant rings are printed on a host dielectric material and made in a periodic or aperiodic fashion.

In this section, the potential use of metamaterials for renewable energy solutions is investigated here. We propose a low-cost, low-profile metamaterial resonant, highly absorbing structure, which will then physically work as an anti-reflective screen at the visible operating spectrum of solar energy radiation. This high absorber structure will be integrated directly with PV solar cells.

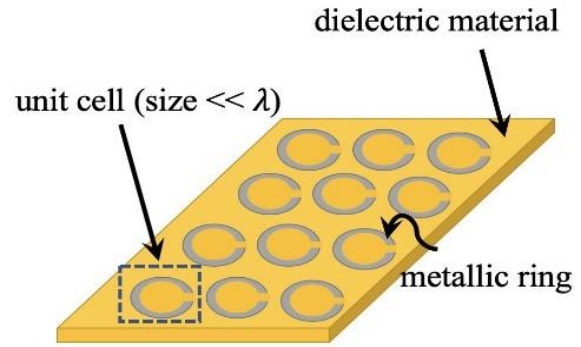


**Figure 5.** Generic view of an engineered metamaterial structure. Note that the grey area represents metallization.

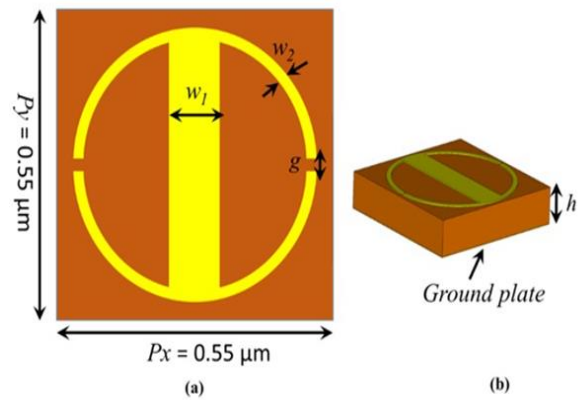


**Figure 6.** The proposed multi-resonant metamaterial absorber unit cell: (a) top view; (b) perspective view. Note that the yellow shaded area represents metallization.

##### 4.1 Proposed multi-resonant metamaterial absorber

Figure 6 depicts the proposed multi-resonant metamaterial absorber. The multi-resonant absorber consists of an electrically very small resonant square unit cell that is shaped in the form of two concentric metallic rings with gaps on opposite sides in order to significantly enhance the resonance of the structure. The rings are made of gold material with a conductivity of  $4.09 \times 10^7$  S/m and a thickness of 4 nm. The resonant unit cell inclusions are then made periodic and printed on a grounded host medium of low-loss Polyimide material with a relative permittivity of  $2.88 - j0.09$  and thickness  $h = 0.12 \mu\text{m}$ . The optimized dimensions for the rest of unit cell parameters (as shown in Figure 6) are:  $P_x = P_y = 0.55 \mu\text{m}$ ,  $w_1 = 0.11 \mu\text{m}$ ,  $w_2 = 0.02 \mu\text{m}$ , and  $g = 0.01 \mu\text{m}$ .

##### 4.2 Proposed PV solar cell with metamaterial absorbing screen

In this section, the potential application of the proposed metamaterial absorbing screen for the efficiency enhancement of PV solar panels is studied next. An



optical study was initially carried out using COMSOL Multiphysics in order to numerically estimate the PV solar panel's absorption strength with and without metamaterial layer as well as electron-hole generation rate for the two aforementioned PV panels cases. After which, the electrical study was conducted to numerically obtain the essential circuit parameters in terms of  $I - V$  and  $P - V$  curves as well as the efficiency of the PV solar panel with and without a metamaterial screen.

It is essential to explore first the effective constitutive parameters of the proposed metamaterial absorbing screen in terms of effective electric permittivity,  $\epsilon_{eff}$ , and effective magnetic permeability,  $\mu_{eff}$ . Such parameters can be extracted from numerically computing scattering parameters from the proposed metamaterial unit cell with the assumption of having a homogenized and periodic structure. Then from the computed effective impedance,  $Z_{eff}$  and refractive index,  $n$ , both  $\epsilon_{eff}$  and  $\mu_{eff}$  can be computed using the below relations. More details about constitutive parameters retrieval of metamaterial structures can be found in (Numan, A. and Sharawi, M. 2013 & Szabó *et al.*, 2010). Figure 7 depicts the numerically retrieved effective constitutive parameters of the proposed metamaterial absorbing structure.

$$\mu_{eff} = n Z_{eff} \quad (7)$$

and

$$\epsilon_{eff} = \frac{n}{Z_{eff}} \quad (8)$$

where  $n$  is the refractive index,  $Z_{eff}$  is the effective impedance of the metamaterial slab,  $\mu_{eff}$  is the effective permeability, and  $\epsilon_{eff}$  is the effective electric permittivity of the metamaterial slab.

Both optical and electrical analyses for a solar cell with and without a metamaterial absorbing screen are considered next. Without loss of generality, amorphous silicon-based solar cell thin film is considered in this work, which belongs to the second-generation solar cells. This is of concern since such materials are mostly the dominant ones in solar PV cells' thin film technology.

Figure 8 depicts the absorption strength of the developed absorbing structure alone as a function of frequency. As shown in Figure 8, a very high absorption strength was achieved, reaching its peak at around 99.5% at 547 THz under TE polarization. Very good agreement can be seen between the results from COMSOL and validated with a similar modelling environment under CST Microwave Studio. Moreover, three peaks from the designed absorber with a good absorption response above 50% can be seen over the visible band. The very minimal discrepancy can be seen above 600 THz, but that is attributed to the variation of the meshing scheme from both simulators.

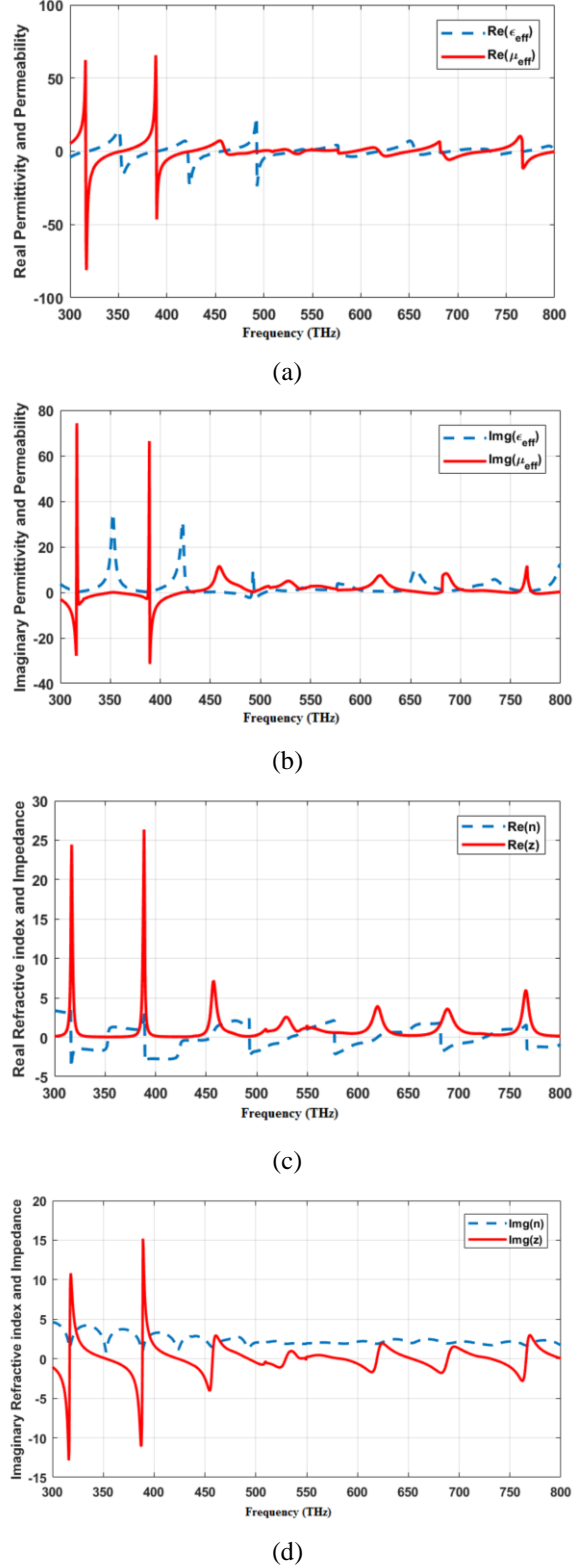


**Figure 7.** Numerical results show the extracted (a) real part of effective permittivity and permeability; (b) imaginary part of effective permittivity and permeability; (c) real part of the effective impedance and refractive index; and (d) imaginary part of the effective impedance and refractive index from the proposed metamaterial absorbing screen.

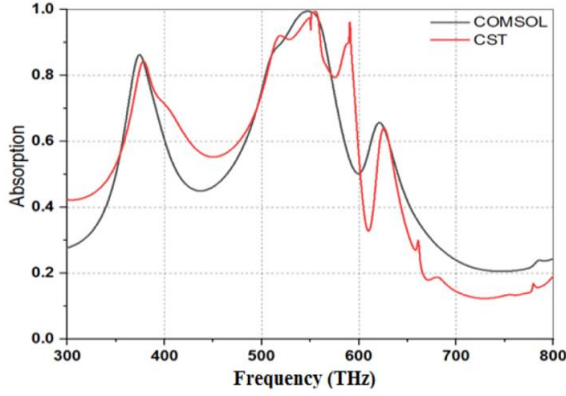


**Figure 8.** Numerically computed results showing the absorption from the developed absorber obtained using COMSOL Multiphysics and validated with CST Microwave Studio.

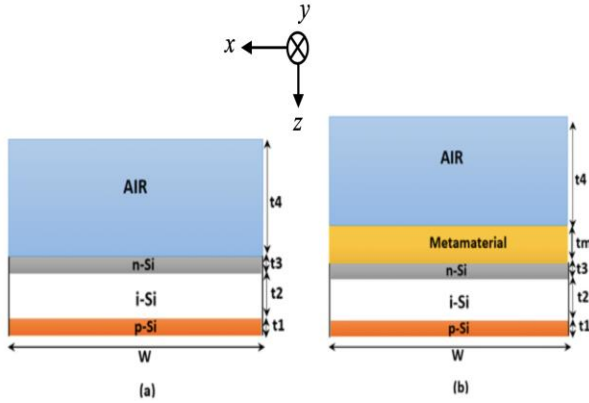


**Figure 9.** 2D view showing (a) PV solar cell structure without metamaterial layer (reference case) and (b) PV cell structure with integrated metamaterial layer.

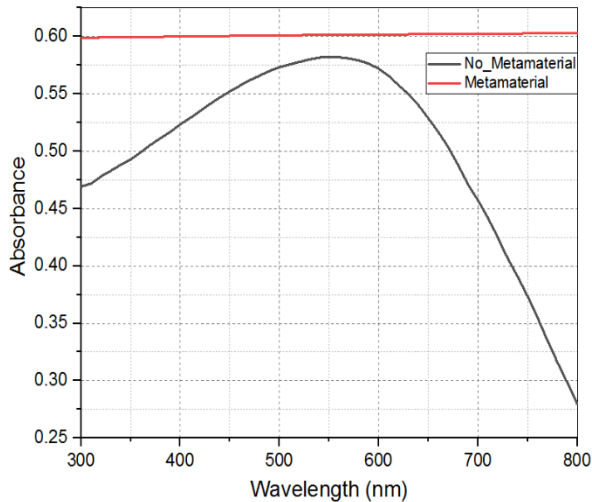


**Figure 10.** Numerical results showing solar cell light absorption with and without the proposed metamaterial absorbing.

**Table 1.** Dimensions of the proposed solar cell with metamaterial absorbing screen.

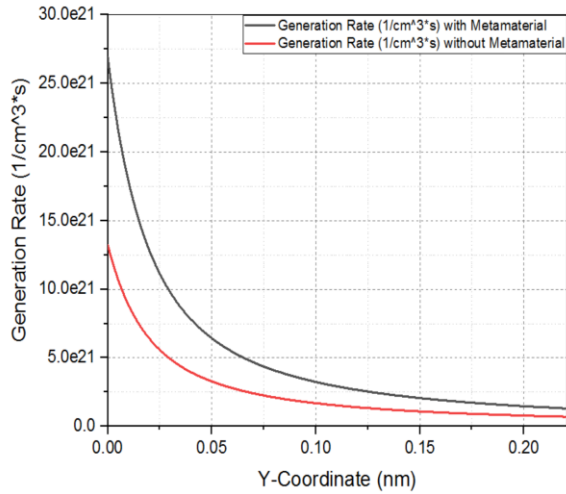
Symbol	Parameters(s)	Value	Unit
W	Solar cell width	0.55	$\mu\text{m}$
$t_1$	the thickness of the p-Si layer	10	nm
$t_2$	the thickness of the i-Si layer	200	nm
$t_3$	the thickness of the Air layer	265	nm
$t_m$	the thickness of the proposed metamaterial screen	0.12	$\mu\text{m}$

Figure 9 shows details of the modelled structure of silicon-based solar cells with and without the proposed metamaterial absorbing screen. Table 1 provides details of the dimensions of the modelled solar cell. Note that the length of the modelled solar cell structures is set to be 1000 nm (i.e., along y-direction, see Figure 9). Standard irradiance with a value of  $100 \text{ mW/cm}^2$  is considered. An input power  $P_{in}$  of  $55.5 \text{ nm}$  was considered within the input parameters to the modelled structure.

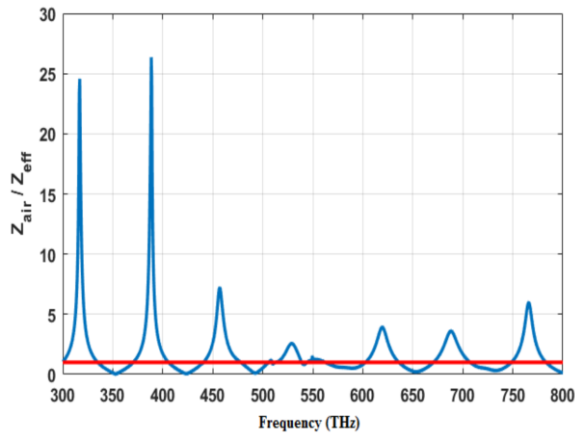
We emphasize here that within the metamaterial absorbing layer in Figure 9, the effective constitutive parameters,  $\epsilon_{eff}$  and  $\mu_{eff}$ , of the retrieved metamaterial absorbing structure have been used to mimic the real metamaterial structure. This was done in order to avoid the high computational time and excessive memory that are needed within the numerical full-wave simulator

Figure 10 depicts numerically computed absorption of the proposed solar cell structure with and without a metamaterial layer. As can be seen from the figure, not only enhancement of absorption is achieved in the case of the solar cell structure with a metamaterial layer, but also flatness of absorption is visible throughout the solar radiation visible spectrum.

Figure 11 shows the generation rate of the proposed solar cell structure with and without the metamaterial layer. The generation rate was numerically calculated using equation (5). Enhancement in generation rate of the proposed solar cell with metamaterial screen is achieved, with almost double growth rate, which is then expected to allow for additional absorption of plasmons' through the absorbent metamaterial layer and hence results in frequency-dependent effective impedance that satisfies the air input impedance.



**Figure 11.** Numerical results show solar cell light generation rate with and without the proposed metamaterial.



**Figure 12.** The Computed ratio of  $Z_{air}/Z_{eff}$ . Note that the red line represents the same ratio of value equals unity.

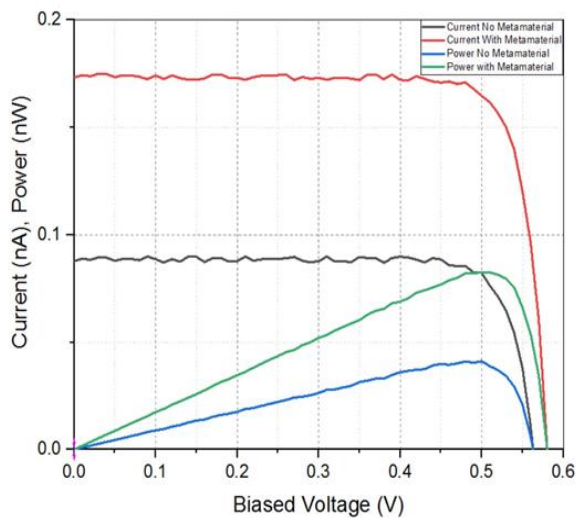


**Figure 13.** Numerical results show I - V and P - V curves for the solar cell with and without the proposed metamaterial absorbing screen.

**Table 1.** Electrical characteristics of the solar cell structure with and without the metamaterial layer.

Symbol	Parameter	Without Metamaterial	With Metamaterial
$V_{oc}$ (V)	open-circuited voltage	0.565	0.580
$I_{sc}$ (nA)	short-circuited current	0.088	0.173
$V_{max}$ (V)	maximum voltage	0.500	0.510
$I_{max}$ (nA)	maximum current	0.0411	0.083
$P_{max}$ (nW)	maximum power	0.0412	0.083
$FF$	filling factor	0.828	0.669
$\eta$ (%)	the efficiency of solar cell	7.4	12

**Table 3.** Performance comparison of the developed efficiency enhancement PV solar cell structure with metamaterials absorber against other structures from the literature.

Reference	Absorption* (%)	Efficiency (%)	Structure complexity
Hamouche, H. and Shabat, M. (2018)	62	-	moderate
Liu <i>et al.</i> , (2012)	84	-	moderate
Lin <i>et al.</i> , (2020)	95	-	moderate
<b>Proposed structure</b>	<b>99.5</b>	<b>12</b>	<b>low</b>

- Absorption is related to the performance of the electromagnetic absorber itself.

Moreover, it is worth noting from Figure 12 that the impedance matching condition ( $Z_{air}/Z_{eff} = 1$ ) occurs at a frequency of 547 THz, which corresponds to the highest energy absorption from the metamaterial layer. As such, an increase in PV solar cell efficiency is permissible within the increased energy absorption.

The electrical study and assessment of the solar cell structure with and without metamaterials are investigated next. Both I - V and P - V curves have been numerically evaluated, as shown in Figure 13, taking into consideration all structure dimensions, thicknesses and losses. Within the numerical full-wave simulation model, excitation of light intensity was assumed to be normal to the PV solar cell structures (i.e., along the z-direction). From such curves in Figure 13, the electrical performance of the solar cell structures with and



without metamaterial layer can be obtained graphically, including  $P_{max}$ ,  $I_{max}$ ,  $V_{max}$ ,  $V_{oc}$  and  $I_{sc}$ . The filling factor and efficiency of the solar cell structures can then be computed

Table 2 illustrates the comparison of the numerically computed parameters for the solar cell structure's electrical performance with and without the metamaterial layer.

Table 3 presents a comparison of our proposed PV solar cell structure with metamaterials against other solar cells with absorbers published in the literature. We can see that the absorption rate of the proposed structure is around 60%, while the absorption from the structure (Hamouche, H. and Shabat, M. (2018)) was 62%, and higher absorption of 84% was reported by the authors in (Liu *et al.*, (2012)) in the visible spectrum.

It is worth noting here that the absorption profile for the developed structure was wideband and flat, covering the visible spectrum. Furthermore, we can see an appreciable increase in the efficiency of the proposed structure, reaching 12% with an enhancement of 4.6%, while efficiency enhancement from earlier studies was not reported. It is also important to highlight here that there are a number of research studies in the literature focusing on solar to thermal efficiency based on the concept of channelling the heat from solar radiation, which is expected to be higher than our reported efficiency for PV solar cells structures.

## 5. CONCLUSION

In this paper, an efficiency enhancement technique for solar cell structures was proposed and numerically evaluated. The composite PV solar cell's structure comprises embedding homogenized engineered metamaterial absorbing screen within PV solar cells. The metamaterial layer behaves as an anti-reflective screen after carefully designing the metamaterial resonant unit inclusion in order to minimally mitigate photons' reflections from the solar cell panel.

Based on the numerical electromagnetic full-wave simulations, efficiency enhancement of the proposed composite PV solar cell was achieved, where efficiency has been enhanced and increased from 7.4% to 12%. This was attainable due to the well-matched effective impedance of the proposed metamaterial screen to that free-space impedance.

Owing to the many features of the proposed metamaterial screen, including its low-profile and cost-effective solution, which can even result in additional features upon the proper design of a unit cell, we believe that applications of metamaterials in solar cells will be very viable in the synthesis, design and manufacturing of new class of smart solar cell structures. In fact, such metamaterial screen can be configured to allow for more advanced features, including reconfigurability, digitally programmable and automated maintenance monitoring. The main goal

of the next phase of this research work is to fabricate the composite metamaterial structure and compare the experimental results with the findings in this paper.

## CONFLICT OF INTEREST

The authors declare that there are no conflicts of interest regarding this article.

## FUNDING

The authors did not receive any funding for this research.

## ACKNOWLEDGMENT

The authors would like to thank Sultan Qaboos University for providing the computing resources to accomplish this work.

## REFERENCES

- Alibakhshikenari, M., Virdee, B., Ali, A., and Limiti, E. (2018), Miniaturised planar-patch antenna based on metamaterial L-shaped unit-cells for broadband portable microwave devices and multiband wireless communication systems. *IET Microwaves, Antennas & Propagation* 12(7): 1080-1086.
- Bagmanci, M., Karaaslan, M., Unal, E., Akgol, O., Bakir, M., and Sabah, C. (2019), Solar energy harvesting with ultra-broadband metamaterial absorber. *International Journal of Modern Physics B* 33(8): 1950056.
- Baqir, M. and Choudhury, P.K. (2019), Design of hyperbolic metamaterial-based absorber comprised of Ti nanospheres. *IEEE Photonics Technology Letters* 31(10): 735-738.
- Basore, P.A. (1990), Numerical modelling of textured silicon solar cells using PC-1D. *IEEE Transactions on electron devices* 37(2): 337-343.
- Biwole, P.H., Eclache, P. and Kuznik, F. (2013), Phase-change materials to improve solar panel's performance. *Energy and Buildings* 62: 59-67.
- Brown, G., Ager, J., Walukiewicz, W., and Wu, J. (2010), Finite element simulations of compositionally graded InGaN solar cells. *Solar Energy Materials and Solar Cells* 94(3): 478-483.
- Ceci, B.R., Pinheiro Bernardon, D., Canha, L. and Santana, T. (2018), "Technology Roadmap Storage: Energy Storage Perspectives," in *Proc. 53<sup>rd</sup> International Universities Power Engineering Conference (UPEC)*. Glasgow, UK, pp. 1-6.
- Chung, H.-H., Tse, K., Hui, S., Mok, C., and Ho, M. (2003), A novel maximum power point tracking technique for solar panels using a SEPIC or Cuk converter. *IEEE Transactions on power electronics* 18(3): 717-724.
- Dincer, F., Akgol, O., Karaaslan, M., Unal, E., and Sabah, C. (2014), Polarization angle independent

- perfect metamaterial absorbers for solar cell applications in the microwave, infrared, and visible regime. *Progress in Electromagnetics Research* 144: 93-101.
- Dong, Y. and Itoh, T. (2012) "Metamaterial-based antennas," *Proceedings of the IEEE*, 100(7): 2271-2285.
- Ferroukhi, R., Khalid, A., Hawila, D., Nagpal, D., El-Katiri, L., Fthenakis, V., and Al-Fara, A. (2016). *Renewable Energy Market Analysis—The GCC Region*. International Renewable Energy Agency: Abu Dhabi, UAE.
- Geisz, J.F., France, R., Schulte, K., Steiner, M., Norman, A., Guthrey, H., Young, M., Song, T., and Moriarty, T. (2020), Six-junction III–V solar cells with 47.1% conversion efficiency under 143 Suns concentration. *Nature energy* 5(4): 326-335.
- Gil, M., Bonache, J. and Martin, F. (2008), Metamaterial filters: A review. *Metamaterials* 2(4): 186-197.
- Green, MA (1987) "High efficiency silicon solar cells," in *Proc. Seventh EC Photovoltaic Solar Energy Conference*. Springer, Dordrecht, pp. 681-687.
- Hamouche, H. and Shabat, M. (2018). "Artificial metamaterials for high efficiency silicon solar cells," In *Processings of the Third International Symposium on Materials and Sustainable Development*, pp. 105-115, July 2018.
- Hohm, D. and Ropp, M. (2000). "Comparative study of maximum power point tracking algorithms using an experimental, programmable, maximum power point tracking test bed," In *Proc. Conference Record of the Twenty-Eighth IEEE Photovoltaic Specialists Conference-2000 (Cat. No. 00CH37036)*, pp. 1699-1702.
- Jiang, Z.H., Gregory, M.D. and Werner, D.H. (2012), Broadband high directivity multibeam emission through transformation optics-enabled metamaterial lenses. *IEEE Transactions on Antennas and Propagation* 60(11): 5063-5074.
- Kalogirou S. (2017), McEvoy's handbook of photovoltaics fundamentals and applications. Academic Press.
- Kshetrimayum, R.S. (2004), A brief intro to metamaterials. *IEEE potentials* 23(5): 44-46.
- Kundtz, N. and Smith, D.R. (2010), Extreme-angle broadband metamaterial lens. *Nature materials* 9(2): 129-132.
- Liu, Y., Chen, Y., Li, J., Hung, T., and Li, J. (2012). Study of energy absorption on solar cell using metamaterials. *Solar Energy* 86: 1586-1599.
- Lin, K., Lin, H., Yang, T., and Jia, B. (2020). Structured graphene metamaterial selective absorbers for high efficiency and omnidirectional solar thermal energy conversion. *Nature communication* 11: 1389.
- Luo, M., Shen, S., Zhou, L., Wu, S., Zhou, Y., and Chen, L. (2017), Broadband, wide-angle, and polarization-independent metamaterial absorber for the visible regime. *Optics express* 25(14): 16715-16724.
- NREL. (2022), Best research-cell efficiency chart from 1976 to the present. National Renewable Energy Laboratory [Online: <https://www.nrel.gov/pv/cell-efficiency.html>, accessed 1 February 2022].
- Numan, A.B. and Sharawi, M. (2013), Extraction of material parameters for metamaterials using a full-wave simulator [education column]. *IEEE Antennas and Propagation Magazine* 55(5): 202-211.
- Saga, T. (2010), Advances in crystalline silicon solar cell technology for industrial mass production. *npg asia materials*, 2(3): 96-102.
- SAOC, OPAWPC, *OPWP's 7-Year Statement, (2018-2024)*. 2018.
- Sathe, T.M. and A. Dhoble (2017), A review on recent advancements in photovoltaic thermal techniques. *Renewable and Sustainable Energy Reviews* 76: 645-672.
- Shchegolkov, D.Y., Azad, A., O'Hara, J., and Simakov, E. (2010), Perfect subwavelength fishnetlike metamaterial-based film terahertz absorbers. *Physical review B* 82(20): 205117.
- Shelby, R.A., Smith, D.R. and Schultz, S. (2001), Experimental verification of a negative index of refraction. *science* 292(5514): 77-79.
- Szabó, Z., Park, G., Hedge, R., and Li, E. (2010), A unique extraction of metamaterial parameters based on Kramers–Kronig relationship. *IEEE Transactions on Microwave Theory and Techniques* 58(10): 2646-2653.
- Veselago, V.G. (1967), Electrodynamics of substances with simultaneously negative  $\epsilon$  and  $\mu$ . *Usp. fiz. nauk* 92: 517.
- Wu, C., Neuner, B., John, J., Milder, A., Zollars, B., Svoy, S., and Shvets, G. (2012), Metamaterial-based integrated plasmonic absorber/emitter for solar thermo-photovoltaic systems. *Journal of Optics* 14(2): 024005.
- Zakharchenko, R., Licea, L., Perez, S., Vorobiev, P., Dehesa, U., Perez, J., Gonzalez, J., and Vorobiev, Y. (2004), Photovoltaic solar panel for a hybrid PV/thermal system. *Solar Energy Materials and Solar Cells* 82(1-2): 253-261.
- Zimmermann, H. (2000) "Basics of optical emission and absorption," in *Proc. Integrated Silicon Optoelectronics*. Springer, 1-10.
- Zhang, J. (2016). *National Renewable Energy Laboratory*.
- Zhu, W., Song, Q., Yan, L., Zhang, W., Wu, P., Chin, L., Cai, H., Tsai, D., Xiang, Z., Deng, T., Ting, S., Gu, Y., Qiang, G., Kwong, D., Yang, Z., Huang, R., Liu, A., and Zheludev, N. (2015). A flat lens with tunable phase gradient by using random access reconfigurable metamaterial. *Advanced Materials* 27(32): 4739-4743.